

Multicenter Structure of the Ground and Excited States of the ${}^9\text{Be}$ Nucleus

M. A. Zhusupov and R. S. Kabataeva

Al-Farabi Kazakh National University, Almaty, 480078 Kazakhstan

e-mail: raushan19860722@mail.ru

Abstract—The relation between states and the [441] and [432] Young diagrams in a many-particle shell model of the ${}^9\text{Be}$ nucleus with possible $\alpha\alpha n$ - and αtd -configurations in the cluster model is established.

DOI: 10.3103/S1062873812040375

INTRODUCTION

The properties of light atomic nuclei can be simulated most completely by the many-particle shell model (MSM) [1]. This model adequately expresses the position of low-lying energy levels and their quantum numbers, the magnitudes of magnetic moments, root-mean-square radii, etc. Within the accountable configurations the wave functions (WF) of the model constitute a complete set of states and satisfy the requirements of the fermionic statistics; i.e., they are antisymmetrized. The MSM thus enables us to consider both nucleonic and cluster degrees of freedom in uniform terms and is therefore highly appropriate for studying diverse nuclear processes. The application of the MSM appears to be especially successful in considering nuclear processes localized within the internal area of a nucleus [2] such as the reactions of quasi-elastic cluster knockout at high transmitted pulses, various reactions involving compound particles significant contributions to whose cross-sections are made by mechanisms of cluster stripping or pick-up, by heavy-particle stripping or cluster substitution, and so on [3]. A study of peripheral processes reveals obvious disadvantages resulting mainly from incorrect asymptotic form of the radial WFs of the model. These processes include, first of all, those of cluster photodisintegration and radiative particle capture. The potential cluster models are better for describing them. These models assume that a nucleus consists of two or three compound particles—d, t, and α particles—and nucleons are in the ground state of their internal motion, whereas all excitations of the nucleus are attributed to the relative motion of fragments. A principal point of these models is the application of cluster-cluster and nucleon-cluster interactions, allowing for the compound structure of particles and reflecting the elastic scattering phases. Generally, no explicit antisymmetrization of the WFs is made in this model, but the Pauli principle is taken into consideration. Deep attraction potentials with forbidden states are therefore used. The structures of allowed and for-

bidden states are determined according to the Levinson generalized theorem [3]. A shell model is used to obtain a WF of the correct form in the potential cluster model. In the αt -cluster model of the ${}^7\text{Li}$ nucleus, the radial WF of the fragments is an oscillatory $R_{3P}(r)$, i.e., it contains one node in the internal region; the WF of the ${}^6\text{Li}$ nucleus is a single-noded $R_{2S}(r)$, and for the ${}^8\text{Be}$ nucleus in the $\alpha + \alpha$ channel and ${}^{16}\text{O}$ in the ${}^{12}\text{C} + \alpha$ channel, we have a binodal function of the $R_{4S}(r)$ type.

THE MULTICLUSTER STRUCTURE OF THE ${}^9\text{Be}$ NUCLEUS

The ${}^9\text{Be}$ nucleus has a specific nuclear structure. Unlike lighter nuclei from a deuteron to ${}^8\text{Be}$, whose WFs in the shell model are more than 95% characterized by one predominant configuration, the ${}^9\text{Be}$ nucleus contains no explicitly singled out components. In the MSM, the WF of the ground state is composed of 13 components [1], the total contribution of the two components with the [441] Young diagram reaching approximately 96%. The contribution of the states having the [432] Young diagram does not exceed three per cent. It is quite obvious that the predominant configuration of the ${}^9\text{Be}$ nucleus is the $\alpha\alpha n$ model [4]. It is this model that best describes the properties of the ${}^9\text{Be}$ nucleus. Only this model yields an apt description of the (γ, p) , (γ, d) , and (γ, t) photonuclear processes on the ${}^9\text{Be}$ nuclear [5] and the hadron elastic scattering reactions at low transmitted pulses [6]. It should be noted that like in the MSM, the WF of the ground state in the $2\alpha n$ model is characterized by three components making approximately equal contributions. The shell configuration with the [432] Young diagram corresponding directly to the $\{\alpha td\}$ cluster decomposition correlates to higher exci-

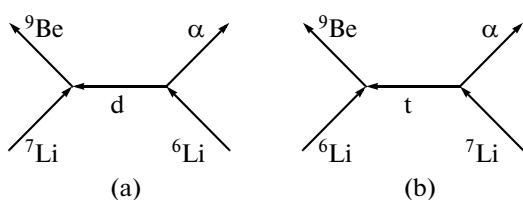


Fig. 1. Diagrams illustrating the reactions of direct (a) deuteron and (b) triton transfer in the lithium nuclei.

tation energies [1]. At the same time, it was suggested in [7] that the indicated states with the [432] Young diagram be searched for in lithium transfer reactions of types ${}^7\text{Li}({}^6\text{Li}, \alpha){}^9\text{Be}$ and ${}^6\text{Li}({}^7\text{Li}, \alpha){}^9\text{Be}$ (see Fig. 1). Owing to the low binding energy of ${}^7\text{Li}$ in the $\alpha + t$ channel and of ${}^6\text{Li}$ in the $\alpha + d$ channel, the predominant mechanisms are in both cases the transfer of the deuteron and triton clusters, respectively. The flexibility of the MSM, however, is that the [441] Young diagram presumes deuteron and triton escape, since

(according to Littlewood's rule) decompositions $[441] \rightleftharpoons [43] + [2]$ and $[441] \rightleftharpoons [42] + [3]$ are possible [7]. For a more comprehensive description of the above mentioned lithium reactions, not only the states of the ${}^9\text{Be}$ nucleus with the [432] Young diagram must be considered, but also the states with the [441] diagram.

The spectroscopic factors in the ${}^6\text{Li} + t$ and ${}^7\text{Li} + d$ channels including both the [441] and [432] Young diagrams were calculated by the authors. In the transfer reactions, the excitation cross section σ of the levels of the residual nucleus (${}^9\text{Be}$ in this case) can be represented by the expression $\sigma \sim (2J+1) \sum_L S_L \Phi$, assuming a direct mechanism in which S_L are corresponding spectroscopic factors and Φ is a factor depending on the kinematic characteristics. Assuming that Φ is a more or less smooth value in dependence on energy, the peaks observed in the reactions must be related to the peaks of the spectroscopic factors.

The calculated values of the spectroscopic factors are shown in Table 1. The same values are presented in

Table 1. Spectroscopic factors of the deuterons and tritons in the ${}^9\text{Be}$ nucleus for its various states

Levels of ${}^9\text{Be}$		S_d^L		S_t^L		$(2J+1) \sum_L S_d^L$	$(2J+1) \sum_L S_t^L$
$\Delta E^*, \text{ MeV}$	J, T	$L=0$	$L=2$	$L=1$	$L=3$	${}^7\text{Li} + d \rightarrow {}^9\text{Be}^*$	${}^6\text{Li} + t \rightarrow {}^9\text{Be}^*$
0–2	3/2, 1/2	3.6×10^{-2}	3.7×10^{-1}	9.0×10^{-2}	8.2×10^{-4}	1.00	1.00
2–3	3, 1	2.3×10^{-2}	8.0×10^{-1}	9.1×10^{-2}	7.5×10^{-2}	2.00	1.93
4–5	3/2, 1/2	4.3×10^{-2}	3.3×10^{-1}	2.8×10^{-2}	2.8×10^{-3}	0.92	0.34
5–6	5/2, 1/2	2.9×10^{-3}	3.9×10^{-1}	3.8×10^{-3}	4.8×10^{-1}	1.44	8.04
6–7	7/2, 1/2		2.2×10^{-1}		3.3×10^{-1}	1.10	7.48
9–10	5, 1	1.7×10^{-1}	1.7×10^{-1}	6.4×10^{-1}	3.3×10^{-2}	0.44	4.46
10–11	5, 1	5.0×10^{-1}	3.0×10^{-1}	6.2×10^{-1}	1.6×10^{-1}	2.36	10.36
11–12	6, 1	5.7×10^{-1}	5.4×10^{-1}	5.5×10^{-1}	1.7×10^{-2}	4.50	9.48
13–14	5/2, 1/2	6.4×10^{-2}	2.6×10^{-1}	6.1×10^{-2}	5.4×10^{-2}	1.19	1.90
14–15	3/2, 1/2	4.1×10^{-2}	2.0×10^{-1}	4.6×10^{-2}	4.8×10^{-2}	0.61	1.04
15–16	5, 1	1.0×10^{-1}	1.4×10^{-1}	1.8×10^{-1}	2.1×10^{-1}	0.54	6.96
17–18	8, 2	1.1×10^{-1}	9.7×10^{-1}	2.1×10^{-1}	4.4×10^{-1}	2.96	9.34
18–19	3/2, 1/2	3.3×10^{-2}	1.9×10^{-1}	1.9×10^{-1}	5.9×10^{-3}	0.55	2.20
19–20	5/2, 1/2	5.4×10^{-3}	1.1×10^{-1}	3.9×10^{-3}	9.0×10^{-2}	0.43	1.49
21–22	13/2, 3/2	4.1×10^{-3}	2.3×10^{-1}	1.3×10^{-2}	1.6×10^{-1}	0.41	3.04
23–24	17/2, 3/2	1.3×10^{-3}	3.3×10^{-2}	4.1×10^{-3}	1.1×10^{-1}	0.13	2.12
24–25	2, 1	2.5×10^{-2}	5.5×10^{-3}	3.8×10^{-2}	3.3×10^{-5}	0.05	1.42

Fig. 2 as histograms comprising the sums of the S -factor values within an energy range of 1 MeV. A comparison with experimental data of [8] shows that the theoretical study correctly represents the main peaks at energies $E = 11.8, 15.2, 17.8$, and 22 MeV. There are also moderate peaks at $E = 0$ and 3 MeV resulting from the [441] Young diagram.

The three-cluster states of α td nature can be correlated not only with the orbital [432] Young diagram but also (with no less certainty) with the [441] Young diagram. It is therefore not surprising that the authors managed to provide a successful description of the (γ , d) and (γ , t) photonuclear processes in the ${}^9\text{Be}$ nucleus by using the $\alpha\alpha n$ -model [5].

NUCLEONIC SPECTROSCOPIC FACTORS FOR THE ${}^9\text{Be}$ NUCLEUS

The calculation results for the spectroscopic S factors of the separation of a neutron from the ground state of the ${}^9\text{Be}$ nucleus, obtained by the authors from the MSM and the cluster $\alpha\alpha n$ -model, are presented in Table 2. The ground $J^\pi = 0^+$ and the first excited 2^+ states of the ${}^8\text{Be}$ nucleus were studied. The experimental data obtained in various reactions of the single-neutron pickup type differ from one another [9, 10] considerably. What they have in common, however, is that the S factor for the transition to the ground state is higher than that for the transition to the excited state. As can be seen from Table 2, this result is inconsistent with calculations according to the MSM [1]. In contrast, the three-body $\alpha\alpha n$ model yields the correct relationship between the S_n factor values for the ground and excited states of the ${}^9\text{Be}$ nucleus [11]. The calculated spectroscopic S factor values for the separation of a proton from the ground state of the ${}^9\text{Be}$ nucleus are given in Table 3. The transitions to the four low-lying states of the ${}^8\text{Li}$ nucleus whose energy positions can be rendered by the MSM [1] are considered in this model. The isospin of the levels of the residual

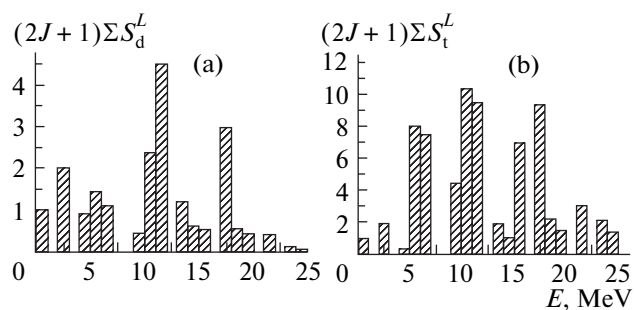


Fig. 2. Excitation spectrum of the ${}^9\text{Be}$ nucleus in reactions (a) ${}^7\text{Li}({}^6\text{Li}, \alpha){}^9\text{Be}$ and (b) ${}^6\text{Li}({}^7\text{Li}, \alpha){}^9\text{Be}$.

nucleus is $T = 1$. It can be seen from Table 3 that the MSM reproduces the experiment quite well. The same is valid for the calculations performed in the three-body $\alpha\alpha n$ model. It is not surprising that the results yielded by the MSM for protons are better than those for neutrons. As has already been mentioned, the main disadvantage of the shell model is the incorrect asymptotic form of the radial functions shrinking too rapidly with distance. It is logical that for the separation of a proton from ${}^9\text{Be}$ ($\varepsilon_{\text{binding}} = 16.9$ MeV), the results obtained for the S factors better match the experimental data, since the protons are more localized in the internal region of the nucleus (where the MSM must work quite well) than the valence weakly bound neutron ($\varepsilon_{\text{binding}} = 1.7$ MeV).

The same picture can also be observed in the case of the S factors for the α particles. The binding energy of the α particles in ${}^9\text{Be}$ is only 2.47 MeV, so the three-body potential model must describe the spectroscopic factors for the α particles better than the MSM. Indeed, the MSM yields equal values of the S factors for $L = 0$ and 2 , and their sum equals 1.12 (see Table 4). At the same time, the three-body potential model yields a figure of 0.67 as the sum of the S factors, which is much closer to the experimental value of $S = 0.63$ [13] than that produced by the MSM.

Table 2. Spectroscopic factors of the neutron separation from the ground state of the ${}^9\text{Be}$ nucleus with the formation of ${}^8\text{Be}(J^\pi, T, E^*)$

J^π, T		S factor			
$E^*_{\text{experimental}}, \text{MeV}$ [10]	$E^*_{\text{theory}}, \text{MeV}$ MSM model [1]	Theory, MSM model [1]	Theory, $2\alpha n$ model	Experiment	
				[9]*	[10]**
$0^+, 0; 0.00$	$0^+, 0; 0.00$	0.54	0.33	0.23	0.55
$2^+, 0; 3.03$	$2^+, 0; 3.00$	0.67	0.26	0.20	0.36

Notes: * From the data according to the (d,t) reaction.

** From the data according to the (p,d) reaction.

Table 3. Spectroscopic factors of the proton separation from the ${}^9\text{Be}$ nucleus with the formation of ${}^8\text{Li}(J^\pi, T, E^*)$

J^π, T		S factor		
$E_{\text{experimental}}^*, \text{MeV}$ [12]	$E_{\text{theory}}^*, \text{MeV}$, MSM model [1]	Theory, MSM model [1]	Theory, $2\alpha n$ model [5]	Experiment [12]
$2^+, 1; 0.00$	$2^+, 1; 0.00$	0.90	0.89	1.07
$1^+, 1; 0.98$	$1^+, 1; 1.10$	0.34	0.33	0.40
$3^+, 1; 2.25$	$3^+, 1; 2.20$	0.33	0.31	0.33
$1^+, 1; 3.21$	$1^+, 1; 3.50$	0.07		0.31

Table 4. Comparison of the S_α factors of the ${}^9\text{Be}$ nucleus calculated by the three-body model with the results obtained by the shell model and the experimental results

Model	S_α	
	$L = 0$	$L = 2$
MSM	0.56 [14]	0.56 [14]
Three-body model	0.52	0.15
Experiment	0.63	

CONCLUSIONS

The ground state of the ${}^9\text{Be}$ nucleus has a wave function with the predominant [441] Young diagram corresponding to a cluster decomposition of $\{\alpha\alpha n\}$ type. The potential three-body model also allows for the channels with neutron, proton, deuteron, triton, and α -particle escape.

The component of the wave function with the [432] Young diagram corresponding to the $\{\alpha td\}$ cluster decomposition is a small addition to the WF of the ground state. In particular, the cluster αtd model does not suggest the neutron escape observed in the experiment and accompanied by the formation of the ground and the first excited states of the ${}^8\text{Be}$ nucleus, whose WFs are characterized by the [44] Young diagram. The states of an αtd nature are for the most part highly excited states of the ${}^9\text{Be}$ nucleus. The observed escape of α particles accompanied by the formation of the ${}^5\text{He}$ nucleus having the [41] Young diagram in its ground state is impossible in the αtd model. Allowing

for the states with the [441] Young diagram in the reactions of triton and deuteron pickup by the ${}^6\text{Li}$ and ${}^7\text{Li}$ nuclei, respectively, considerably widens the excitation spectra in the lithium transfer reactions.

REFERENCES

1. Boyarkina, A.N., *Struktura yader 1p obolochki* (Structure of 1-Shell Nuclei), Moscow: Mosk. Gos. Univ., 1973.
2. Neudachin, V.G. and Smirnov, Yu.F., *Nuklonnye assotsiatsii v legkikh yadrakh* (Nucleon Associations in Light Nuclei), Moscow: Nauka, 1966.
3. Nemets, O.F., Neudatchin, V.G., Rudchik, A.T., et al., *Nuklonnye assotsiatsii v atomnykh yadrakh i reaktsii mnogonuklonnykh peredach* (Nucleon Clustering in Nuclei and Multinucleon Transfer Reactions), Kiev: Naukova Dumka, 1988.
4. Voronchev, V.T., et al., *Yad. Fiz.*, 1994, vol. 57, p. 1964.
5. Burkova, N.A., Zhaksybekova, K.A., and Zhusupov, M.A., *Phys. Part. Nucl.*, 2005, vol. 36, no. 4, p. 427.
6. Zhusupov, M.A. and Ibraeva, E.T., *Phys. Part. Nucl.*, 2000, vol. 31, no. 6, p. 723.
7. Lebedev, V.M., Neudachin, V.G., and Sakharuk, A.A., *Phys. At. Nucl.*, 2000, vol. 63, no. 2, p. 195.
8. Glukhov, Yu.A., et al., *Yad. Fiz.*, 1971, vol. 13, p. 277.
9. Goncharov, S.A., et al., *Czech. J. Phys. B*, 1988, vol. 38, p. 12.
10. Zaika, N.A., et al., *Yad. Fiz.*, 1984, vol. 39, p. 1081.
11. Zhusupov, M.A., Kaipov, T.D., and Sakhiev, S.K., *Izv. Akad. Nauk, Ser. Fiz.*, 1996, vol. 60, no. 1, p. 123.
12. Ajzenberg-Selove, F., *Nucl. Phys. A*, 1988, vol. 490, p. 1.
13. Kurath, D., *Phys. Rev. C*, 1973, vol. 7, p. 139.
14. Wang, C.W., et al., *Phys. Rev. C*, 1980, vol. 21, p. 1705.

SPELL: 1. ok